Study of the adsorption of an organic pollutant onto a microporous metal organic framework

Mansouri Taki Eddine Mohammed, Nibou Djamel, Trari Mohamed and Samira Amokrane

ABSTRACT

In this study, the microporous metal organic framework-5 (MOF-5) has been synthesized to be used to remove methyl orange by adsorption. The adsorption experiments exhibit a good adsorption capacity at a catalyst dose of 0.1 g L^{-1} and for an initial concentration of 200 mg L^{-1}, whereas the performance is stable over a wide pH range. The equilibrium adsorption data showed a sigmoidal course, which is well fitted by the Dubinin-Astakhov model applicable for physical adsorption processes ($E = 0.055$ kJ mol^{-1}) onto heterogeneous surfaces and a more homogeneous pore structure ($n = 9.9$), with a maximum adsorption capacity of 1248.35 mg g^{-1}. As can be observed from the evaluation of the kinetic data, the surface of the adsorbent is heterogeneous with different active sites for methyl orange (MO) adsorption. Moreover, based on the rate constant, it can be suggested that there is a specific interaction like electrostatic interaction between MO and the adsorbent for rapid and high uptake of the dye, whereas the adsorption phenomenon is reversible. According to the adsorption mechanisms, intra-particle and film diffusion models simultaneously controlled the rate sorption, which was confirmed by the calculated intra-particle diffusion and the film diffusion coefficients. The evaluation of the thermodynamic parameters revealed that the MO adsorption is spontaneous, endothermic and the randomness increases with the adsorption of MO.

Key words | adsorption, kinetic, mass transfer, microporous MOF-5, organic pollutant, sigmoidal isotherm

Mansouri Taki Eddine Mohammed
(corresponding author)
Nibou Djamel
Samira Amokrane
Laboratory of Materials Technology, Faculty of Mechanic and Engineering Processes,
USTHB,
BP 32, El-Alia, Bab-Ezzouar, 16111 Alger,
Algeria
E-mail: *taki86seg@gmail.com*

Trari Mohamed
Laboratory of Storage and Valorization of Renewable Energies, Faculty of Chemistry,
USTHB,
BP 32, El-Alia, Bab-Ezzouar, 16111 Alger,
Algeria

HIGHLIGHTS

- MOF-5 was synthesized, and with 1248 mg/g exhibits the best adsorption capacity for methyl orange (MO).
- The various parameters influencing the adsorption of MO were optimized, whereas the performance is stable over a wide pH range.
- Equilibrium data showed a sigmoidal course, which better followed the Dubinin-Astakhov isotherm.
- MOF-5 may be applied in the adsorptive removal of anionic dye from contaminated water.

doi: 10.2166/wst.2020.566

GRAPHICAL ABSTRACT

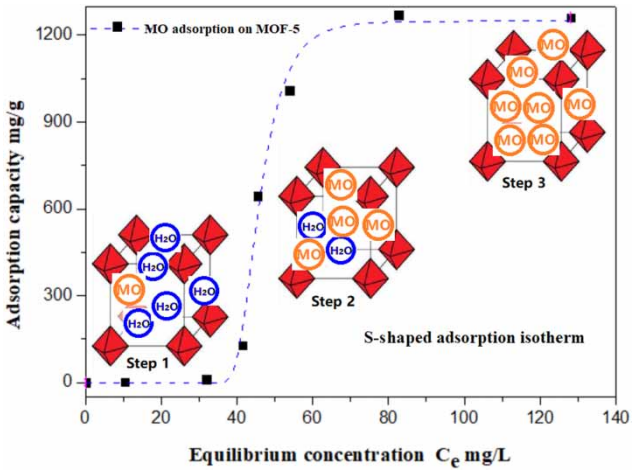

INTRODUCTION

As a result of the global industrial development, water pollution has become a serious threat and critical for the environment (Michael *et al.* 2013). Two percent of the dyes produced are usually discharged into aquatic systems as effluents without any control (Khan *et al.* 2013). The dyes' removal from contaminated water is important because even a small amount is undesirable and dramatically affects the ecosystem by weakening the light intensity, thus blocking the photosynthetic process. Moreover, many dyes employed nowadays are considered to be highly toxic and even carcinogenic (Michael *et al.* 2013). Methyl orange (MO) is a well-known acidic/anionic dye belonging to the azo groups, widely used in the textile, printing, paper, food and pharmaceutical industries (Mittal *et al.* 2007). The presence of azo group ($N=N$) on MO and its low biodegradability make it an issue for the environmental science (Mittal *et al.* 2007). Therefore, its elimination from water is an important necessity owing to its high toxicity (Mittal *et al.* 2007; Chen *et al.* 2010). For the dyes removal, many physical, chemical and biological methods have been used (Chen *et al.* 2010) and thus, adsorption is considered competitive because it's efficient, economically feasible, and requires a simple design (Chen *et al.* 2010). This is possible by exploring novel and efficient materials introduced as adsorbents, which has important practical significance and wide application prospects for environmental protection (Singh & Arora 2011).

Metal organic frameworks (MOFs) are the result of the reaction between organic and inorganic species; they can be described as an organization of secondary units and exhibit a crystalline porous structure (Lee Kim & Ahn 2013). Compared to the traditional porous materials, MOFs possess numerous interesting and appealing features, including a large internal surface area and pore volume, perfectly ordered and well defined pore structures, functionalized pore surfaces, and adjustable pore dimensions (Bao *et al.* 2016). In addition, the structural diversity present in MOFs as new materials has greatly expanded their applications (Khan *et al.* 2013; Fang *et al.* 2018). They are the most studied molecular materials, since they are porous coordination polymers with a great potential for different applications (Khan *et al.* 2013; Ramanayaka *et al.* 2019). Among the applications that have received considerable attention, is the adsorption behavior characteristics of metal–organic frameworks from both fundamental aspects and practical water treatment applications (Khan *et al.* 2013; Fang *et al.* 2018).

The stability of MOFs upon exposure to humidity or aqueous environments is one of the most important barriers to applying several types of MOFs in practical water treatment applications (Tan *et al.* 2015). Among many widely investigated water-sensitive MOFs, particularly built up from carboxylate acid ligands (Tan *et al.* 2015), MOF-5, is a well-known MOF made up by Zn_4O clusters linked by the conjugated base of terephthalic acid (Eddaoudi *et al.* 2002). In fact, the stability of MOF-5 under such conditions is a topic of renewed interest. Rodriguez *et al.* showed that the

exposure of MOF-5 to water produces a relatively stable new phase, MOF-5 W, which slowly transforms to more stable phase MOF-5H, a mixture of MOF-5 W and zinc terephthalate dihydrate (ZTDH) (Rodríguez *et al.* 2015).

The main objective of this study was to evaluate the efficiency of MOF-5, which is considered water sensitive in practical applications of water treatment. As applications, using MOF-5 to remove MO by adsorption in an aqueous environment, the effect of operating parameters like the contact time, the pH, the temperature, the initial dye concentration and catalyst loading on the adsorption were investigated, it was after the synthesis of metal organic framework-5 and defined using different characterization techniques. Equilibrium, kinetic, mass transfer and thermodynamic studies were also performed with this purpose.

MATERIAL AND METHODS

Synthesis and characterizations of MOF-5

All chemicals used in this work were of analytical grade quality purchased from Merck and applied without any purification. MOF-5 was synthesized according the method reported elsewhere (Mueller *et al.* 2006; Lee *et al.* 2013). Briefly, a mixture of 9.65 g of zinc nitrate tetrahydrate $Zn(NO_3)_2$ $4H_2O$ and 2.05 g of terephthalic acid (BDC) $C_8H_6O_4$ were dissolved in 297 mL of dimethylformamide (DMF) C_3H_7NO as organic solvent and homogenized under moderate stirring at ambient conditions. Then, the solution was agitated in a glass reactor equipped with a reflux condenser and heated at 130 °C for 4 h. After 1 h and slow cooling, white crystals of MOF-5 emerged; the precipitate was filtered and immersed in DMF (100 mL) overnight. It was filtered again and immersed in chloroform $CHCl_3$ (150 mL). The solvent was changed three times over 7 days. Finally, the obtained powder was activated for 3 h at 60 °C under a reduced pressure (~0.2 mbar).

The MOF-5 sample was characterized by X-ray diffraction (XRD) using a Bruker D8-Advance instruments operating at 40 kV and equipped with CuK_α ($\lambda = 1.5405$ A) radiation, at a scan rate of 1°/min and 2θ step size of 0.02°. The morphology of the crystalline powder was analyzed with a scanning electron microscope (SEM). Fourier transformed infrared spectroscopy (FT-IR), in the range (400–4,000 cm^{-1}) using a Bruker ALPHA one FT-IR-ATR spectrometer to identify the functional groups. The N2 adsorption/desorption isotherms were obtained at liquid N2 temperature of 77 K using a Micromeritics ASAP 2010 system.

Batch adsorption study

An aqueous stock solution (1,000 mg L^{-1}) was prepared by dissolving methyl orange (MO: $C_{14}H_{14}N_3NaO_3S$, molecular weight: 327.33, Merck, 99.5% dye content) in distilled water. MO solutions at different concentrations (10–250 mg L^{-1}) were prepared by successive dilution. The MO removal experiments with MOF-5 were carried out in batch mode in Erlenmeyer flasks (150 mL capacity) under magnetic stirring. The pH of the solution was adjusted with HCl or NaOH (1 N). A known mass of MOF-5 (adsorbent dose) was added to the solution, and stirred for a pre-defined time. The effect of temperature on the adsorption of MO was carried out in a double walled Pyrex reactor (capacity 200 cm^3) connected to a thermo-static bath. To monitor the adsorption kinetics, samples were taken at various time intervals and the adsorbent was separated from the mixture by centrifugation (3,000 rpm, 3 min), The solution was used for the measurement of MO concentration after dilution (if necessary) using a UV-Vis spectrophotometer (Optizen 2120 UV-Visible, $\lambda_{max} = 465$ nm). The percentage removal of MO was calculated from the relation:

$$\text{Removal of MO}(\%) = \frac{(C_0 - C_e)}{C_0} \times 100 \quad (1)$$

The adsorption capacity of adsorbent material per unit mass at any time, q_t (mg g^{-1}) was calculated by the relation:

$$q_t = \frac{C_0 - C_t}{M} \times V \quad (2)$$

where C_0 (mg L^{-1}) is the initial MO concentration, C_e (mg L^{-1}) the equilibrium concentration, C_t (mg L^{-1}) the concentration in time t of MO, V(L) the volume of the solution, and M(g) the weight of MOF-5.

RESULTS AND DISCUSSION

Characterization

The XRD pattern of MOF-5 (Figure 1(a)) agrees with that reported elsewhere (Hafizovic *et al.* 2007; Rodríguez *et al.* 2015; Jiang *et al.* 2016). The synthesized samples still exhibit several characteristic peaks of MOF-5, and the crystal faces could still be found, such as (200), (220), (400), (420) (Jiang *et al.* 2016). The important diffraction peaks of MOF-5 are observed at ($2\theta = 8.8°$) with the presence of

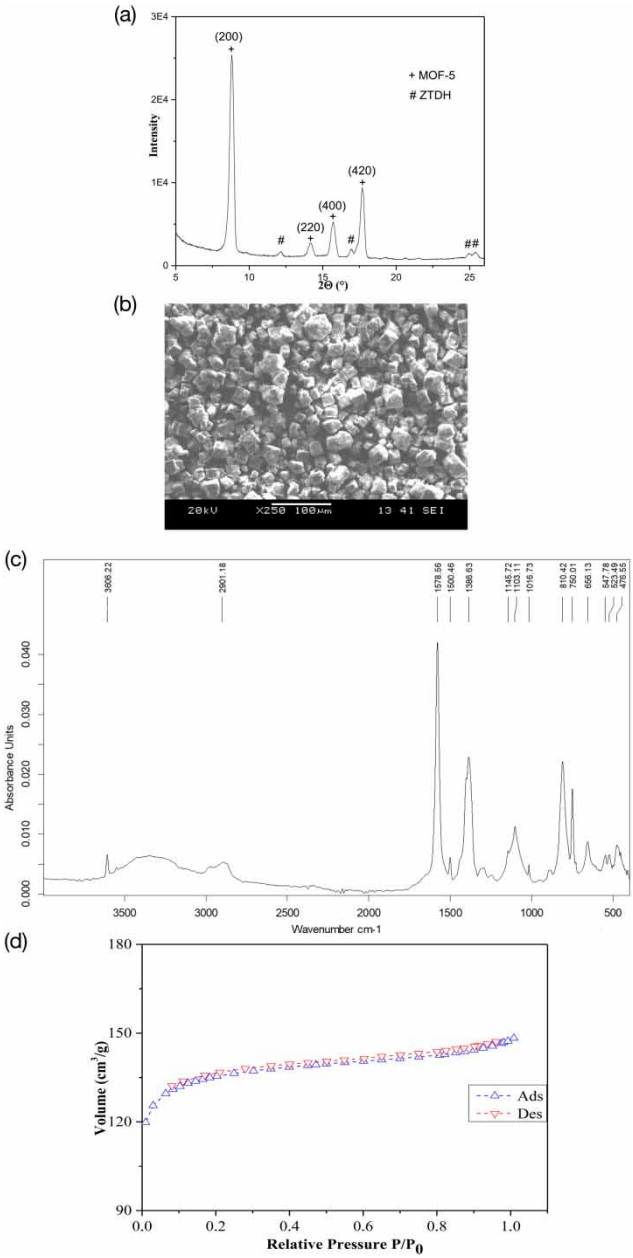

Figure 1 | Characterization data for synthesized MOF-5: (a) XRD pattern; (b) SEM image; (c) FTIR; (d) N_2 adsorption-desorption isotherm.

peaks (marked with hashtags) indicating the presence of zinc terephthalate dihydrate ZTDH (Rodríguez *et al.* 2015).

The morphology of MOF-5 was studied by SEM analysis and the micrographs were taken with different magnifications (Figure 1(b)) indicate a cubic morphology and with an average size of 20 μm.

The FT-IR spectra for the synthesized MOF-5 (Figure 1(c)) confirmed the presence of several functional groups whose characteristic bands at 1,386 and 1,578 cm^{-1} correspond to the asymmetric and symmetric stretching of the C-O bond of the carboxylate group directly bonded to Zn (Zhang *et al.* 2019). The small bands in the region (656–1,145 cm^{-1}) are assigned to the C-H group of the benzene ring of terephthalic acid. The characteristic peak at 500 cm^{-1} is caused by Zn-O vibration (Iswarya *et al.* 2012). Furthermore, the wide band (3,390 and 3,606 cm^{-1}) and the sharp narrow peak are attributed to the O-H group of adsorbed water. This indicates the presence of humidity that is frequently located in the metal coordination, due to its high specific surface area (Phan *et al.* 2010).

The BET surface area was measured by N_2 adsorption/desorption at 77 K (Figure 1(d)). As can be observed, the MOF-5 exhibits a microporous nature with an isotherm of type I (Langmuir type) adsorption without hysteresis, according to the IUPAC classification and this indicates that our adsorbent has a microporous nature. As derived from the adsorption data, the properties of the porous structure of MOF-5 are summarized in Table 1.

Adsorption study

Parametric study on MO uptake from aqueous solution

Effect of contact time. The contact time is an important parameter for practical application. The results (Figure 2(a)) show that MO uptake by MOF-5 is rapid in the first 15 min, reaching ~53% of the total MO removal, with the adsorption capacity reaching ~260 mg g^{-1} due to the large surface area of the adsorbent (BET surface area = 532.86 m^2 g^{-1}), and then reaching equilibrium after 30 min. This observation is due to the number of available sites for adsorption of MO being large in the initial step and tends to saturation (Bakhtiari & Azizian 2015). The rapid uptake of dye molecules from aqueous solution indicates the efficiency of the adsorption process and the advantage of the use of this adsorption system in effluent decolorization.

Effect of pH. The influence of pH on the MO adsorption was investigated over a broad pH range (3–10); Figure 2(b) shows that the maximum adsorption percentage and capacity of MO are obtained at pH ~3 (74.53% and 279.5 mg g^{-1} resp.). However, with increasing pH both the percentage and adsorption capacity decrease slightly to

Table 1 | N_2 adsorption properties of MOF-5

Sample	BET surface area	Micropore volume	Pore size
MOF-5	532.86 m^2/g	0.21 cm^3/g	~0.89 nm

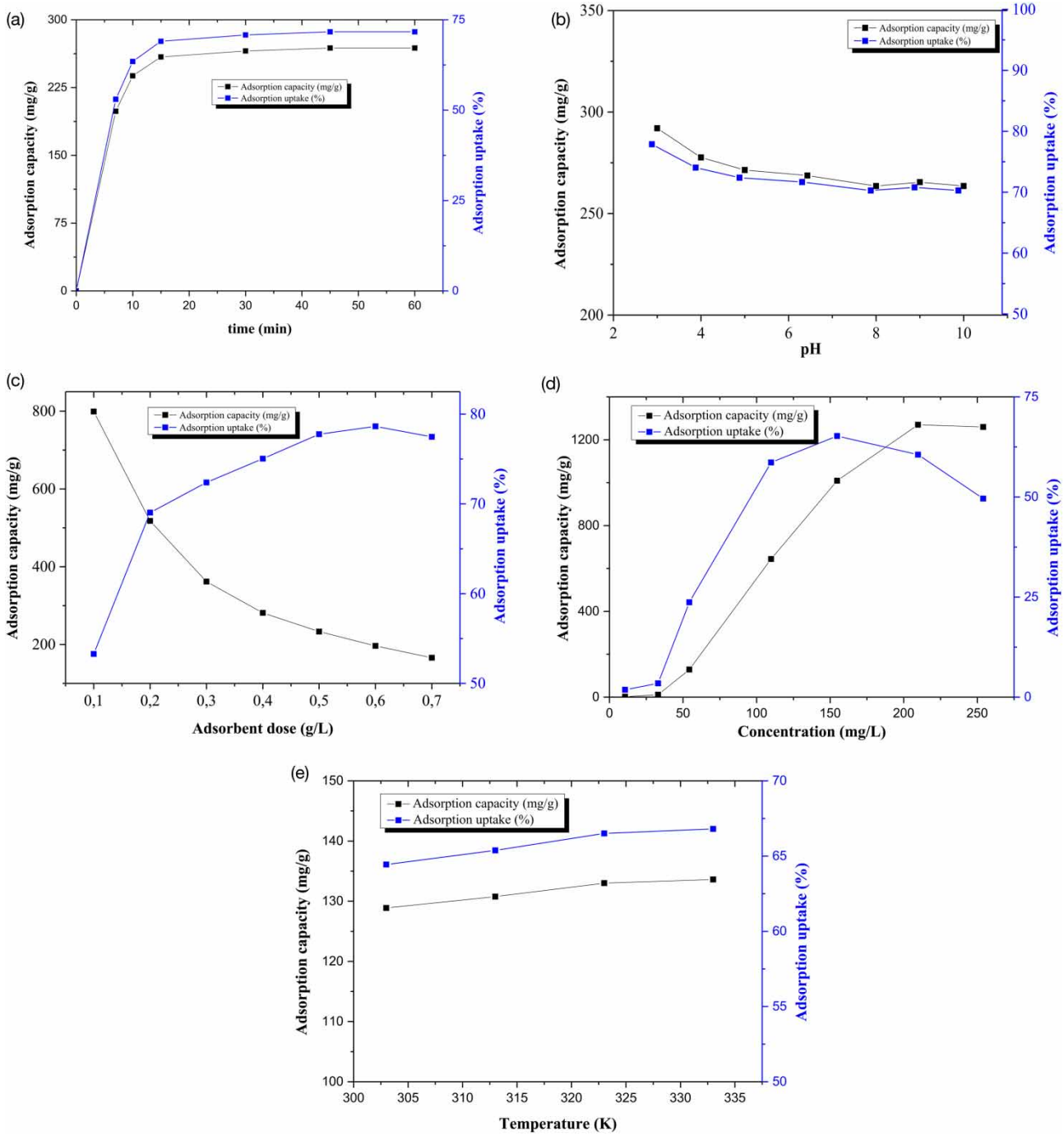

Figure 2 | Effect of operating parameters on the adsorption uptake and capacity of MO onto MOF-5: (a) contact time, (b) initial pH, (c) adsorbent dose, (d) initial concentration of MO and (e) temperature.

reach 70.3% and 263.5 mg g^{-1} at pH ~10. This is due to the positive charge of the adsorbent MO, which decreases with increasing pH. The maximum adsorption at lower pH may be due to the electrostatic attractions between negatively charged functional groups of MO and the positive charge of the adsorbent surface (Mittal *et al.* 2007; Gu *et al.* 2014). Hydrogen ions also act as a bridging ligand between the adsorbent and MO molecules (Gu *et al.* 2014). At high pH, the adsorbent acquires a negative charge and no hydrogen bonds can be formed between MO and the MOF-5 surface.

In this case, only the Van der Waals force contributes to MO adsorption.

Effect of the adsorbent dose. The adsorption is mainly a surface phenomenon and the adsorbent dose is a significant parameter. The surface available for the adsorption process, and consequently the MOF-5 dose, can considerably affect adsorption efficiency. Its influence on the MO adsorption was examined by the addition of different doses (0.1–0.6 g L^{-1}) to 100 mL of MO (Figure 2(c)). The MO removal increases to 78.6% when raising the MOF-5 dose to 0.6 g L^{-1} and remains almost unchanged thereafter. However, the amount of MO adsorbed, q_t (mg g^{-1}), decreased from 619.53 to 196.6 mg g^{-1}. This is due to the high number of unsaturated sorption sites during the adsorption process.

Effect of initial concentration of MO. The influence of the MO concentration on adsorption is determined by fixing the dose of MOF-5 (0.1 g L^{-1}) and taking a different MO dye concentrations ranging between 10 and 250 mg L^{-1}. Figure 2(d) shows clearly three distinct steps of adsorption: The first step, the adsorption capacity and the MO removal efficiency are weak; in the second step the adsorption capacity *qe* (mg g^{-1}) increases from 11.37 to 1,270.8, when the C_0 increases from 30 to 200 mg L^{-1} and the MO removal efficiency increases from 3.4 to 60.6%. Finally, in the third step, the adsorption capacity value reaches a plateau for the higher concentrations, while the MO removal efficiency decreases. Therefore, it can be said that the weak of adsorption capacity and the MO removal efficiency in low concentrations can be explained by the lack of adsorption affinity for MO on the surface of MOF-5, by the fact that water adsorption is more important than MO on MOF-5, because of the nature of MOF-5 and smaller size of the water molecule, which expands the hydrogen bonding network and fills the free space more easily than MO. After reaching a certain concentration, the adsorption of MO is increased due to adsorbent-adsorbent cooperative interactions. This leads to the formation of multilayer adsorption through van der Waals reactions and competitive water substitution. However, in the third step the MO removal efficiency decreases, which may be due to the fact that at higher initial concentrations of the MO dye, the number of MO dye molecules is greater than the number of MOF-5 surface sites available for adsorption.

Effect of temperature. The thermal effect on the removal of MO by MOF-5 has been studied in series of experiments that were carried out in the range (303–333 K) (Figure 2(e)). The amount of MO adsorbed and the percentage removal increases only slightly from 128.87 mg g^{-1} and 64.4% to 133.6 mg g^{-1} and 66.8% with raising the temperature, indicating an endothermic process. Such results can be explained by the increased solution viscosity, leading to improved exposure to active adsorption sites, on the one hand, and on the other hand the increase of the intraparticle diffusion rate (Mekatel *et al.* 2015).

Adsorption isotherms

For the solid-liquid system, the equilibrium is an important physico-chemical aspect in the adsorption mechanism (Barkat *et al.* 2015). In this work, the four models of Langmuir, Freundlich, Toth, Temkin, Dubinin-Radushkevich (D-R) and Dubinin-Astakhov isotherms (Table 2) were tested to investigate the relationship between the amount of MO adsorbed by MOF-5 and their equilibrium

Table 2 | Isotherm models of adsorption

Isotherm model	Non-linear equation	Reference
Langmuir	$q_e = \frac{q_m K_L C_e}{1 + K_L C_e}$ (3)	Laib *et al.* (2019)
Freundlich	$q_e = K_F C_e^{\frac{1}{n}}$ (4)	Laib *et al.* (2019)
Toth	$q_e = q_m \frac{b_T C_e}{\left[1 + (b_T C_e)^{\frac{1}{n}}\right]^n}$ (5)	Bakhtiari & Azizian (2015)
Temkin	$q_e = \left(\frac{RT}{b_T}\right) \ln A_T C_e$ (6)	Laib *et al.* (2019)
Dubinin-Radushkevich	$q_e = q_m exp\left(-\beta\left[RT \ln\left(1 + \frac{1}{C_e}\right)\right]^2\right)$ (7)	Laib *et al.* (2019)
Dubinin-Astakhov	$q_e = q_m exp\left(-\left[\frac{RT}{E} \ln\left(1 + \frac{1}{C_e}\right)\right]^n\right)$ (8)	Inglezakis (2007)

concentration in aqueous solution (Figure 3). The results gathered in Table 3 display the non-linear fitting along with the corresponding constant and correlation coefficient (R^2). The non-linear regression analysis of the isotherm models was performed with the Origin Pro 9 software running on Windows 10 platform.

According to the R^2 values and resemblance of the theoretical q_e^{cal} and experimental q_e^{exp} values, these indicate that the Dubinin-Astakhov model gave a good fit with the MO adsorption isotherms onto the MOF-5. The obtained value of $\boldsymbol{n} = 9.9$ was consistent with the reported $\boldsymbol{n}$ range (1–35) of the Dubinin-Astakhov model (Wood 2001), an indication of the homogeneity of the MOF-5 pore structure in comparison to other materials. For instance, the exponent values proposed are $n > 4$ for zeolites, $n = 2$–3 for homogeneous carbons, and $n < 2$ for heterogeneous active carbons. As has been pointed out, $\boldsymbol{n}$ values depend on both the adsorbate and the adsorbent and it is very difficult to have a universal exponent (Inglezakis 2007). The adsorption energy E gives information about the chemical or physical properties of the sorption. The calculated adsorption energy value of adsorption of the MO by MOF-5 is very small ($E = 0.055$ KJ mol$^{-1} < 8$ kJ mol^{-1}) and this implies that the type of adsorption is physical. In this model, q_m represents the maximum adsorption capacity, C_e is the equilibrium concentration of solute in the solution, E is the free energy for a given adsorbate-adsorbent system, which is related to pore dimensions, and the exponent $\boldsymbol{n}$ is the degree of heterogeneity of the micropore system. It is characteristic of the adsorbent, and related to its structure; the more homogeneous the pores the greater its value (Inglezakis 2007). R (KJmol^{-1} K^{-1}) is the universal gas constant and T (k) is temperature.

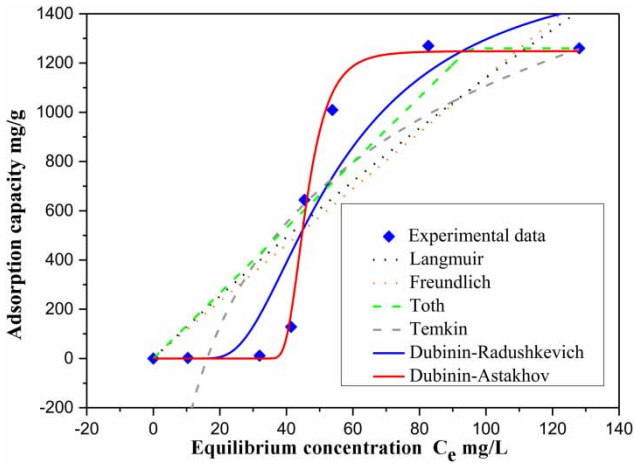

Figure 3 | Comparison of experimental and predicted adsorption isotherms MO dye onto MOF-5 according to Langmuir, Freundlich, Toth, Temkin, Dubinin-Radushkevich and Dubinin-Astakhov models.

Adsorption kinetics

The adsorption study was undertaken to evaluate both the efficiency of the process and the rate limiting step that controls the adsorption uptake of MO onto MOF-5, and it also aids in determining the overall reaction time. To determine the MO adsorption mechanism; that is, the transfer and chemical reaction, the pseudo first order, pseudo second order, elovich, intra-particle diffusion and film diffusion models were tested for MO adsorption as a function of time (Table 4). The plots of model form are shown in Figures 4 and 5, while the determined constants are presented in Tables 5 and 6.

As seen in Table 5, the pseudo first and the pseudo second order models exhibited relatively higher values of R^2, which are superior to 0.97. However, it should be mentioned that the correlation coefficients $\boldsymbol{R^2}$ corresponding to the pseudo first order kinetic model were higher in comparison with the pseudo-second order kinetic model for high concentrations. In addition, the calculated $\boldsymbol{q_e^{cal}}$ from the pseudo-first order kinetic mode were in excellent compliance with the experimental $\boldsymbol{q_e^{exp}}$. It can imply that the adsorption phenomenon at high concentration is reversible (Ahmaruzzaman & Reza 2015), which

Table 3 | The Langmuir, Freundlich, Toth, Temkin, Dubinin-Radushkevich and Dubinin-Astakhov isotherms constants values of MOF-5 adsorbent

Isotherm model	q_{max} (mg·g^{-1})	K_L (L·mg^{-1})	K_F (L·g^{-1})	n	E_a (kJ·mole^{-1})	A_T (L·mg^{-1})	b_T (KJ·mol^{-1})	R^2
Langmuir	9,310.7	0.0014	–	–	––	–	–	0.715
Freundlich	–	–	117.76	1.965	–	–	–	0.508
Toth	1,259.68	–	–	0.0105	–	–	0.00606	0.706
Temkin	–	–	–	–	–	0.0618	4.076	0.704
Dubinin-Radushkevich	1,636.69	–	–	–	0.036	–	–	0.879
Dubinin-Astakhov	1,248.35	–	–	9.904	0.055	–	–	**0.992**

Table 4 | Kinetic models of adsorption

Kinetic model	Non-linear equation	Reference
Pseudo-first-order	$q_t = q_e(1 - e^{-k_1 t})$ (9)	Simonin (2016)
Pseudo-second-order	$q_t = \frac{q_e^2 k_2 t}{1 + q_e k_2 t}$ (10)	Simonin (2016)
Elovich	$q_t = \frac{1}{b}\ln(abt)$ (11)	Wu *et al.* (2009)
Intra-particle diffusion	$q_t = k_{int} t^{0.5} + c$ (12)	Suteu & Malutan (2013)
Film diffusion	$Bt = -0.4977 - \ln(1 - F)$ For $F > 0.85$ (13) $Bt = \left(\sqrt{\pi} - \sqrt{\pi - \left(\frac{\pi^2 F}{3}\right)}\right)^2$ For $F < 0.85$ (14) Where $F = \frac{q_t}{q_e} = 1 - \frac{6}{\pi^2}\sum_{n=1}^{\infty}\frac{1}{n^2}exp(-n^2 Bt)$ (15)	Tsibranska & Hristova (2011)

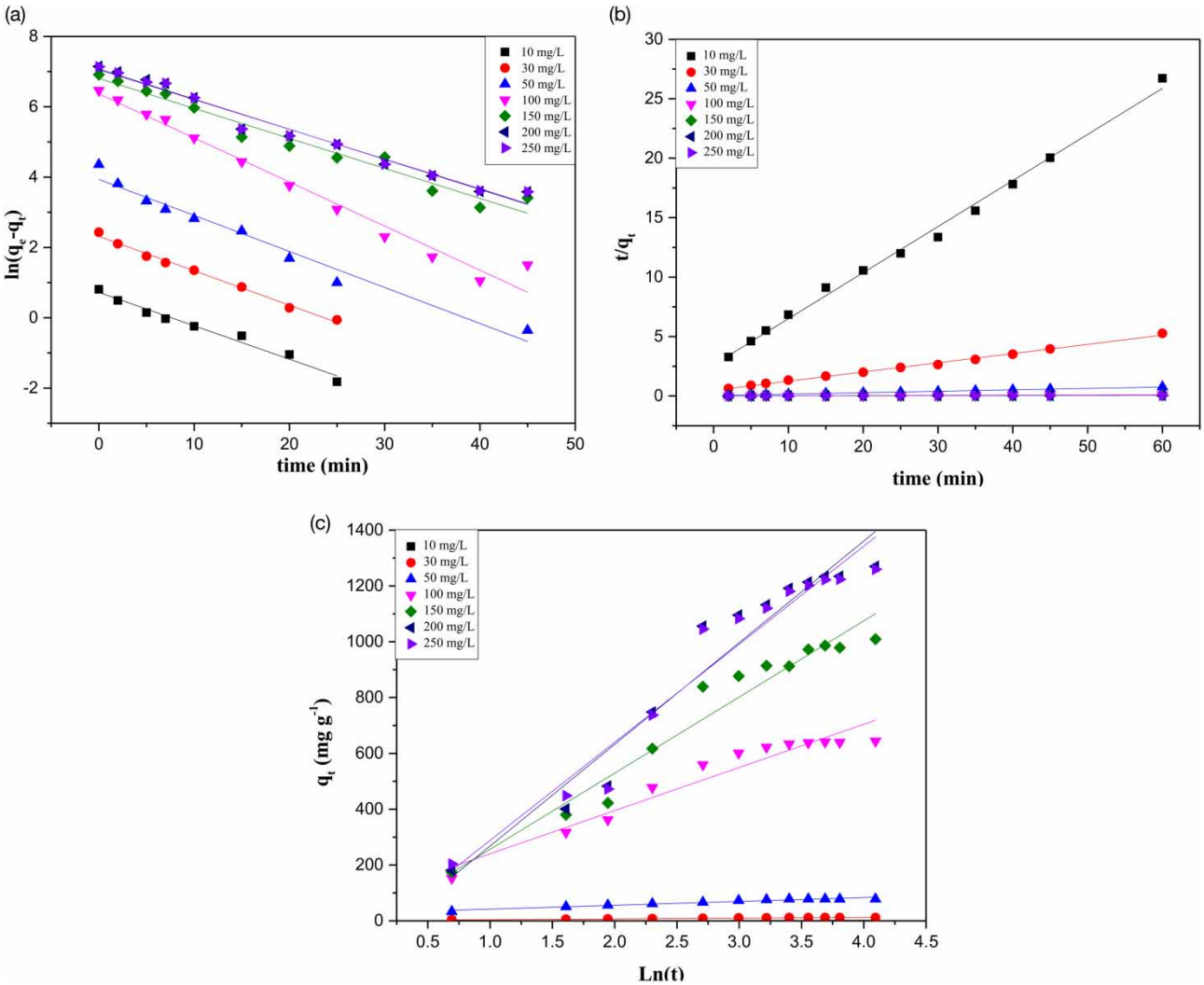

Figure 4 | Kinetic plots of the (a) pseudo-first-order, (b) pseudo-second-order, and (c) Elovich models.

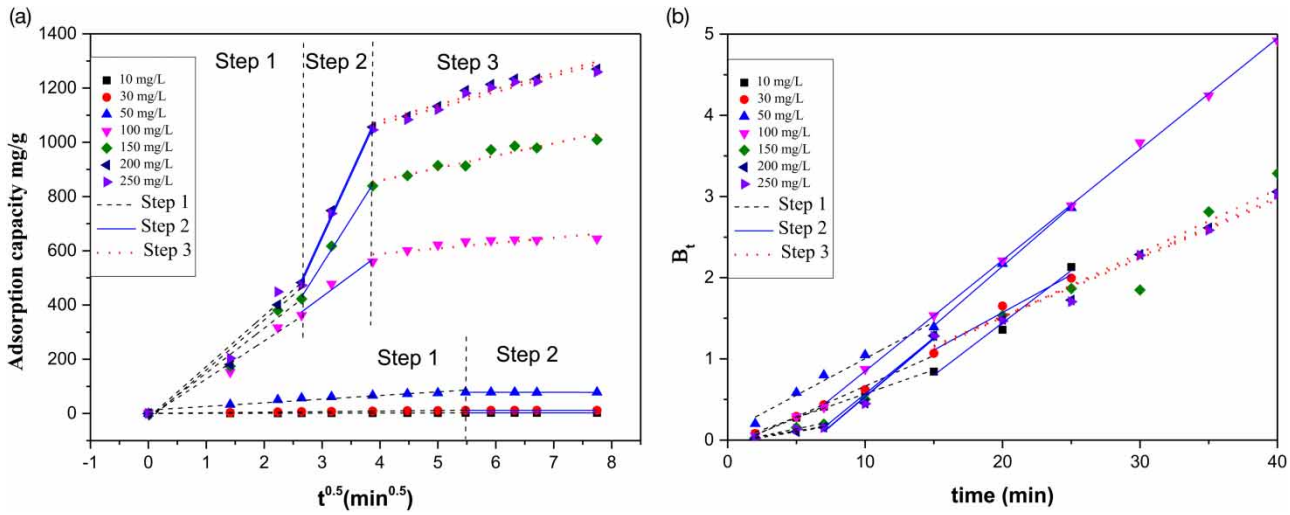

Figure 5 | Mass transfer mechanisms. (a) Intra-particle diffusion and (b) film diffusion models for MO adsorption onto the MOF-5 at different initial MO concentrations.

Table 5 | Parameters of the kinetic models for the adsorption of MO on MOF-5 under different initial concentrations

		Pseudo-first-order (PFO)			Pseudo-second-order (PSO)			Elovich model		
C_o (mg/L)	$q_{e.exp}$ (mg/g)	$q_{e.cal}$ (mg/g)	K_1 (min^{-1})	R^2	$q_{e,cal}$ (mg/g)	K_2 (g/mg min)	R^2	a (mg/g min)	b (g/mg)	R^2
10	2.24	2.1	0.095	0.975	2.6	5.72E-02	0.994	0.85	1.857	0.969
30	11.37	10.1	0.098	0.992	12.9	1.26E-02	0.996	4.71	0.374	0.967
50	78.22	51.2	0.102	0.967	83.5	3.86E-03	0.999	105.69	0.072	0.947
100	644.01	583.1	0.125	0.976	724.6	2.47E-04	0.994	268.96	6.46E-03	0.930
150	1,009.35	904.6	0.085	0.962	1,215.7	8.25E-05	0.987	256.78	3.66E-03	0.947
200	1,270.21	1,181.2	0.086	0.975	1,608.6	4.97E-05	0.974	279.83	2.74E-03	0.940
250	1,259.68	1,154.6	0.085	0.976	1,558.0	5.65E-05	0.980	293.45	2.84E-03	0.941

means that the adsorption mechanism is subject to physical absorption between layers.

As for the low concentrations, the pseudo second order kinetic model gave a better fit, which may indicate that the adsorption mechanism involves electrostatic interactions between the adsorbent and the first layer of adsorbate, and may be considered a chemisorption process (Vargas *et al.* 2011; Laib *et al.* 2019). As can be observed from the Elovich results in Table 5, which exhibited the highest values of R^2 for the low concentrations compared to the high concentrations. The latter is used to describe chemical adsorption on heterogeneous surfaces (Wu *et al.* 2009).

The modeling of the data obtained by the intra-particle diffusion model reveals a correlation of multi-linearity, as shown in Figure 5(a). This proves the presence of more than one sequential step in the adsorption phenomenon (Haddad *et al.* 2018). The k_{int} and C parameters corresponding to each step are reported in Table 6. According to Weber's model (intra-particle diffusion model), the non-null values of the intercept C indicate that during adsorption of MO onto MOF-5 not only is the intra-particle diffusion controlled by them, but also by other diffusion processes. Moreover, if the $\boldsymbol{C}$ values are equal to zero (the plots that pass by the origin), this indicates the adsorption is controlled by the intra-particle diffusion (Suteu & Malutan 2013; Wakkel *et al.* 2019). One can see from the data of Table 6 that with increasing concentration, the boundary effects represented by the intra-particle diffusion constant $\boldsymbol{C}$ increase (Suteu & Malutan 2013), whereas the intra-particle rate constant $\boldsymbol{k_{int}}$ also increases with an increase of concentration. This in turn illustrates an enhanced rate of adsorption (Haddad *et al.* 2018). Moreover, the opposite variation of these two parameters shows that the mass transfer was controlled at the beginning of MO adsorption by a fast intra-

Table 6 | Rate parameters of intra-particle diffusion model and film diffusion model for MO uptake on MOF-5

	Intra-particle diffusion model										Film diffusion model									
	Step 1			Step 2			Step 3				Step 1			Step 2			Step 3			
C_o (mg/L)	k_{int} (mg g^{-1} min$^{-1/2}$)	C (mg·g^{-1})	D (cm^2 s^{-1})	k_{int} (mg g^{-1} min$^{-1/2}$)	C (mg·g^{-1})	D (cm^2 s^{-1})	k_{int} (mg·g^{-1} min$^{-1/2}$)	C (mg·g^{-1})	D (cm^2 s^{-1})	Intercept	B (slope)	D_f (cm^2 s^{-1})	Intercept	B (slope)	D_f (cm^2 s^{-1})	Intercept	B (slope)	D_f (cm^2 s^{-1})
10	0,406	0,092	2,3E-09	–	2.25	–	–	–	–	−0.021	0.059	6.0E-09	−1.134	0.129	1.3E-08	–	–	–
30	2,076	0,560	1,5E-09	–	11.38	–	–	–	–	−0.088	0.075	7.6E-09	−0.283	0.093	9.4E-09	–	–	–
50	13,471	12,590	4,9E-10	–	78.49	–	–	–	–	0.103	0.090	9.1E-09	−0.795	0.147	1.5E-08	–	–	–
100	140,20	−12,76	1,4E-09	158.06	−43.61	5.3E-09	19.53	511.34	8.0E-11	−0.079	0.070	7.1E-09	−0.518	0.137	1.4E-08	–	–	–
150	165,45	−16,29	1,5E-09	337.89	−464.12	9.8E-09	45.60	676.87	1.8E-10	−0.034	0.034	3.5E-09	−0.812	0.138	1.4E-08	−0.065	0.079	8.0E-09
200	184,32	−24,00	1,6E-09	465.15	−738.71	1.2E-08	58.12	847.82	1.8E-10	−0.036	0.028	2.8E-09	−0.898	0.144	1.5E-08	0.063	0.073	7.4E-09
250	188,43	−15,51	1,6E-09	465.15	−749.26	1.2E-08	58.35	835.26	1.9E-10	−0.019	0.027	2.7E-09	−0.901	0.143	1.5E-08	0.066	0.072	7.3E-09

particle diffusion process followed by a slow combination diffusion process. In addition, the horizontal portions of the plot reflect that intra-particle diffusion started to slow down and the adsorption of MO reached equilibrium (Haddad *et al.* 2018).

Boyd's model (film diffusion model) is based on the assumption that particle diffusion is not the sole rate-controlling process. So kinetic data is analyzed using this model (Figure 5(b) and Table 6), in order to identify the rate-limiting step involved in the MO adsorption film diffusion and intra-particle diffusion. The Boyd model is applied by plotting the fractional approach to equilibrium F and time t (Tsibranska & Hristova 2011). As shown in Figure 5(b), the plotted values of B against the experimental values of t present multi-linearity correlation that reveals the existence of more than one sequential step in the adsorption phenomenon (El-Khaiary & Malash 2011). We can also see plots with two linear segments (with one breakpoints) for the concentrations from 10 to 100 mg L^{-1}, and plots with three linear segments (with two breakpoint) for the high concentrations. Whereas the first plots of any concentration and the last plots of high concentration are very near to passing through the origin (see the intercept value from Table 6). According to Boyd's model (El-Khaiary & Malash 2011), film diffusion is not the sole controlling step, whereas intra-particle diffusion is considered more rate-controlling. This finding strengthens the above results of the intra-particle diffusion model.

The intra-particle diffusion coefficient $\boldsymbol{D}$ (cm^2 s^{-1}) and the film diffusion coefficient $\boldsymbol{D_f}$ (cm^2 s^{-1}) were often adopted in order to determine more comprehensively the diffusion mechanisms and to better evaluate the predominant limiting diffusion step. Both coefficients can be estimated from the two following equations (Equations (16) and (17)) (Tsibranska & Hristova 2011):

$$K_{int} = 6\frac{q_e}{r}\sqrt{\frac{D}{\pi}} \tag{16}$$

$$B = \frac{\pi^2 D_f}{r^2} \tag{17}$$

where $\boldsymbol{B}$ is the rate coefficient (slope of equations (13) or (14)) and $\boldsymbol{r}$ is the particle radius of the adsorbent, assuming spherical shape.

To consider that the intra-particle diffusion is rate limiting, the intra-particle diffusion coefficient $\boldsymbol{D}$ should be ranged between 10^{-11} and 10^{-13} cm^2 s^{-1}(Karthikeyan *et al.* 2010). As for whether the film diffusion coefficient $\boldsymbol{D_f}$

is in the interval of 10^{-6}–10^{-8} $cm^2\,s^{-1}$ then film diffusion can be considered as the rate controlling phenomenon (Karthikeyan *et al.* 2010). As shown in Table 6, the calculated value of the intra-particle diffusion coefficient D is high in the range of $D \geq 10^{-11}$, as the film diffusion coefficient D_f values are low in the range of $D_f \leq 10^{-8}$. Consequently, and based also on the intercept values (Table 6), it can be declared here that the adsorption processes of MO on MOF-5 are controlled by both film and intra-particle diffusion steps, this latter being more significant.

Thermodynamic study

The thermodynamic parameter changes in standard enthalpy (ΔH°_{ads}), entropy (ΔS°_{ads}), and free energy (ΔG°_{ads}) due to the transfer of unit mole of solute from solution onto the solid–liquid interface, which helps to highlight the mechanism of the MO adsorption. The thermodynamic parameters (Table 7) are determined from the following equations (Mekatel *et al.* 2019):

$$\Delta G^{\circ}_{ads} = -RT \ln K_c \tag{18}$$

$$\Delta G^{\circ}_{ads} = \Delta H^{\circ}_{ads} - T\Delta S^{\circ}_{ads} \tag{19}$$

where $\mathbf{K_c}$ is the equilibrium constant is calculated by the following relation:

$$K_c = \frac{(C_0 - C_e)}{C_0} \tag{20}$$

The experiments were carried out from 303 to 318 K for MO concentration of 100 mg L^{-1}, and the values of ΔH°_{ads} and ΔS°_{ads} were obtained from the slopes and intercepts of linear regression of the $\boldsymbol{lnK_c}$ versus $\boldsymbol{1/T}$ curve (Equation (21)) (Figure 6):

$$\ln K_c = \left(\frac{\Delta S^0}{R}\right) - \left(\frac{\Delta H^0}{RT}\right) \tag{21}$$

Table 7 | Thermodynamic parameters for the adsorption of MO onto MOF-5 at different temperatures

	Thermodynamic parameters		
T (K)	ΔG° (kJ/mol)	ΔH°(kJ/mol)	ΔS°(kJ/mol)
303	−4.574	3.071	15.107
313	−4.725		
323	−4.8764		
333	−5.0275		

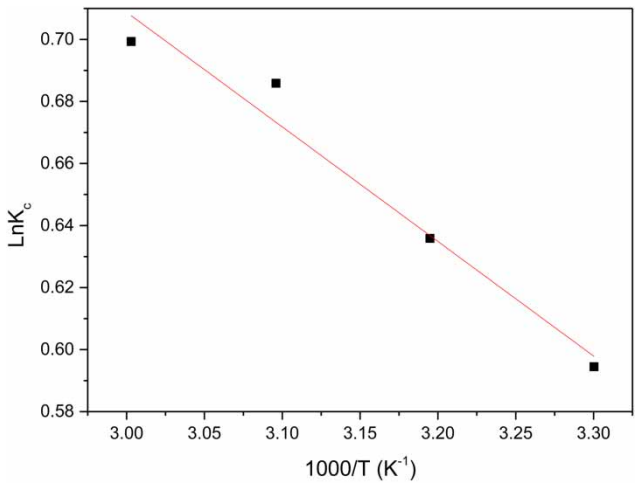

Figure 6 | Plot of ln K_c as a function of *1/T* ($C_0 = 100$ mg L^{-1}, adsorbent dose = 0.5 g L^{-1} and pH ~ 6.3).

The negative value of ΔG°_{ads} for all temperatures indicates that MO adsorbed onto MOF-5 is spontaneous and it was also observed that with increasing temperature, ΔG°_{ads} decreases, indicating that adsorption becomes thermodynamically more favorable. The positive ΔH°_{ads} further confirms the endothermic nature of the MO adsorption, while the value of ΔH°_{ads} is very small. This may be due to a little desorption of pre-adsorbed water. Supporting this assumption, the positive entropy of ΔS°_{ads} means increased randomness of the MO adsorption at the solid-solution interface, probably because of the displacement of water molecules sorbed on the solid surface (which is released into the bulk solution). Also the value of ΔG°_{ads} and ΔH°_{ads} suggests that adsorption is a physisorption process.

Regeneration study

The stability of MOF-5 was investigated by means of recycling experiments, different solvents were tested (Figure 7(a)) such as H_2O, 5% solutions of NaOH, H_2SO_4, NaCl and 5–50% CH_3OH. The desorption of MOF-5 was done in the most efficient eluent (CH_3OH 50%) for three adsorption/desorption cycles (Figure 7(b)). As can be observed in Figure 7(b), there was loss of MO removal efficiency during the third cycle process. The reduction of MO removal efficiency can be explained by the following reasons: (1) there was inevitable loss of adsorbent during the whole adsorption/desorption process; (2) the adsorbed fraction of contaminant on the surface of the adsorbent inhibited the interaction of MOF-5 and MO; (3) there is a possibility of deteriorating structure of the MOF-5.

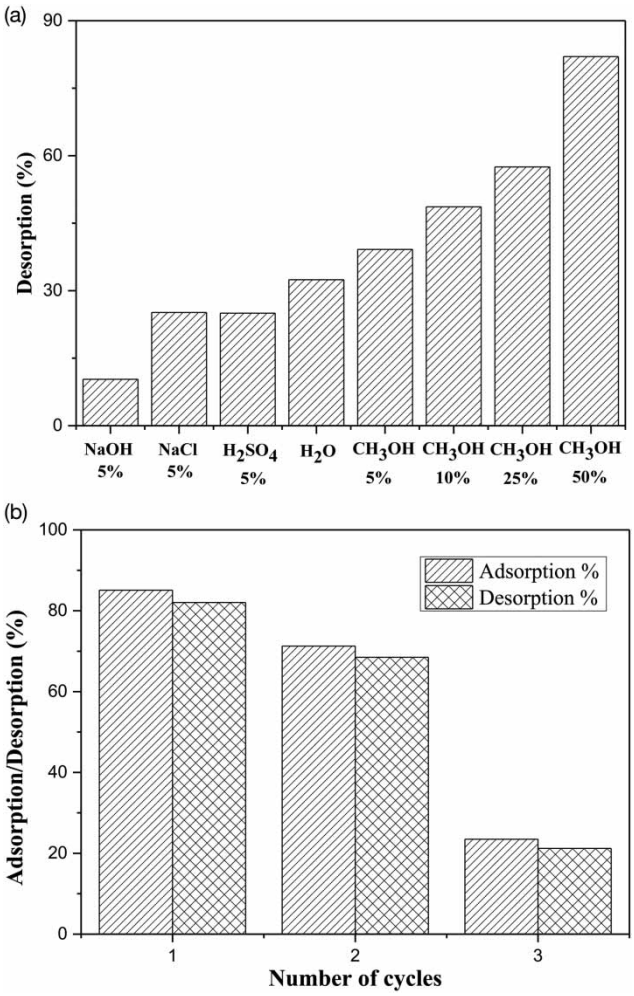

Figure 7 | (a) Desorption of MO using different eluents, (b) MO removal efficiencies of recycled MOF-5.

Comparison of the adsorption of MO on various adsorbents

In this comparison, the maximum adsorption capacities of MO were pooled by different absorbents at the optimum condition in which it occurred, like the pH, adsorbent dose required, initial concentration and the results of the equilibrium isotherm, kinetic, and thermodynamic parameters. Comparing the q_{max} values of MO adsorption onto MOF-5, our adsorbent exhibits a high adsorption capacity ($q_{max} = 1{,}248.35\ mg\ g^{-1}$) at pH of the solution within a high initial concentration of dye of 200 mg/L and a very low adsorbent dose, this comparison revealed that MOF-5 is a promising adsorbent for the removal of organic dyes. Moreover, the adsorption equilibrium is well fitted by the Dubinin-Astakhov model, suggesting that MO adsorption is a physical adsorption process (free energy $E = 0.055\ kJ\ mol^{-1}$) onto MOF-5 heterogeneous surfaces and in the presence of a more homogeneous pore structure ($\boldsymbol{n} = 9.9$). This is also shown in Table 8. The values of k_L, k_1 and k_2 determined from the adsorption of MO onto MOF-5 have high value in almost all cases compared to other studies. Therefore, not only did MOF-5 take up large amounts of the dye, but it also adsorbed MO quickly. However, it should be mentioned that the pseudo-first-order kinetic model fitted well the adsorption of MO onto MOF-5. This can imply that the adsorption phenomenon is reversible, and the value of ΔG° and ΔH° also confirmed that adsorption is a physisorption process. An additional advantage of MOF-5 is that preparation is economic as MOFs are synthesized by 'one-pot' solvothermal methods under mild conditions. Herein, we report a facile route for low cost and low temperature synthesis of MOFs. However, the higher adsorption capacity of the adsorbents may compensate for the cost for such a process.

CONCLUSION

The adsorption of MO onto microporous MOF-type materials has been studied. The adsorption capacity ($1{,}248.35\ mg\ g^{-1}$) and adsorption kinetic constant of MOF-5 have high values in almost all cases compared to other studies, showing the importance of porosity and pore size for adsorption. The results of equilibrium studies show a sigmoidal course (S-shaped), identical to type V, which is well fitted by the Dubinin-Astakhov model applicable for physical adsorption processes (free energy $\boldsymbol{E} = 0.055\ kJ\ mol^{-1} < 8\ kJ\ mol^{-1}$) onto heterogeneous surfaces and a more homogeneous pore structure ($\boldsymbol{n} = 9.9$). Based on the rate constant (pseudo-second or pseudo-first-order kinetics for adsorption) and adsorption capacity, it can be suggested that there is a specific interaction like electrostatic interaction between MO and the adsorbent for rapid and high uptake of the dye. As can be observed from the evaluation of the kinetic data suggested by PFO, PSO and Elovich, the surface of the adsorbent is heterogeneous with different active sites for the MO adsorption. Whereas the adsorption phenomenon at high concentrations is reversible, as for the low concentrations, the data indicate that the adsorption mechanism involves electrostatic interactions between the adsorbent and the first layer of adsorbate. The adsorption mechanisms were well described by both internal and external diffusion models, in which it was found that intraparticle diffusion was the main controlling step. In addition,

Table 8 | Comparison of the results, isothermal, kinetic, thermodynamic parameters and the optimal MO adsorption conditions on different adsorbents

Adsorbents	q_m (mg/g)	pH	R (g/L)	C (mg/L)	Isotherm model	K_L (L/mg)	Kinetic model	K_1 (min^{-1})	K_2E-04 (g/mg min)	ΔH° (kJ/mol)	ΔS° (kJ/mol)	Reference
MOF-5	**1,248.35**	**free**	**0.1**	**200**	**D-A**	0.0014	**PFO**	**0.086**	**0.497**	**3.071**	**15.107**	**This work**
MCM-41	1,000	2	0.3	30	L	0.029	PSO	0.056	57	–[a]	–[a]	Albayati *et al.* (2017)
GO-PANI	885	6	0.6	100	L	–	PSO	–	–	–	–	Wang *et al.* (2018)
UMLDH	715.44	4	0.166	100	L	0.016	PSO	0.11	0.09	–[a]	–[a]	Mu'azu *et al.* (2019)
CMLDH	708.15	4	0.166	100	L	0.014	PSO	0.10	0.15	–[a]	–[a]	Mu'azu *et al.* (2019)
MOF-235	477	2	0.1	20	L		PSO	–[a]	7.67	99.6	131.42	Haque *et al.* (2011)
BDHP-Mt	238.1	free	1.6	400	L	0.1694	PSO	0.027	9.6	61.64	81.51	Gu *et al.* (2014)
PED-MIL101Cr	194	2	0.2	30	L	–[a]	PSO	–[a]	2.75	29.5	62.28	Haque *et al.* (2010)
NH_2-MIL101Al	188	5.6	0.5	30	–[a]	–[a]	PSO	8.7E – 03	1.3	0.489	74.3	Haque *et al.* (2014)
ED-MIL101Cr	160	5.6	0.2	30	L	–[a]	PSO	–[a]	1.06	–[a]	–[a]	Haque *et al.* (2010)
MSBC	173.61	5	2	600	L	0.1266	PSO	0.0457	5	–[a]	–[a]	Zhang *et al.* (2017)
MIL101Cr	114	5.6	0.2	30	L	–[a]	PSO	–[a]	9.01	4.00	35.76	Haque *et al.* (2010)
MIL53Cr	57.9	5.6	0.2	30	L	–[a]	PSO	–[a]	7.23	–[a]	–[a]	Haque *et al.* (2010)

[a]Not determined; L: Langmuir; D-A: Dubinin-Astakhov.

according to the calculated intra-particle diffusion coefficient and the film diffusion coefficient, one can consider that intra-particle diffusion was associated with the control of film diffusion phenomenon. The adsorption of MO over MOF-5 at various temperatures shows that the adsorption is spontaneous and endothermic and the randomness increases with the adsorption of MO. The driving force of MO adsorption over MOF-5 is mainly due to an entropy effect rather than an enthalpy change. Finally, this study demonstrates the efficiency of microporous MOF-type materials that are sensitive to water in practical water treatment applications, and provides a feasible route to prepare efficient MOFs adsorbent for environmental treatment.

DATA AVAILABILITY STATEMENT

All relevant data are included in the paper or its Supplementary Information.

REFERENCES

Ahmaruzzaman, M. & Reza, R. A. 2015 Decontamination of cationic and anionic dyes in single and binary mode from aqueous phase by mesoporous pulp waste. *Environmental Progress & Sustainable Energy* **34** (3), 724–735.

Albayati, T. M., Alwan, G. M. & Mahdy, O. S. 2017 High performance methyl orange capture on magnetic nanoporous MCM-41 prepared by incipient wetness impregnation method. *Korean Journal of Chemical Engineering* **34** (1), 259–265.

Bakhtiari, N. & Azizian, S. 2015 Adsorption of copper ion from aqueous solution by nanoporous MOF-5: a kinetic and equilibrium study. *Journal of Molecular Liquids* **206**, 114–118.

Bao, Z., Chang, G., Xing, H., Krishna, R., Ren, Q. & Chen, B. 2016 Potential of microporous metal–organic frameworks for separation of hydrocarbon mixtures. *Energy & Environmental Science* **9** (12), 3612–3641.

Barkat, M., Nibou, D., Amokrane, S., Chegrouche, S. & Mellah, A. 2015 Uranium (VI) adsorption on synthesized 4A and P1 zeolites: equilibrium, kinetic, and thermodynamic studies. *Comptes Rendus Chimie* **18** (3), 261–269.

Chen, S., Zhang, J., Zhang, C., Yue, Q., Li, Y. & Li, C. 2010 Equilibrium and kinetic studies of methyl orange and methyl violet adsorption on activated carbon derived from *Phragmites australis*. *Desalination* **252** (1–3), 149–156.

Eddaoudi, M., Kim, J., Rosi, N., Vodak, D., Wachter, J., O'keeffe, M. & Yaghi, O. M. 2002 Systematic design of pore size and functionality in isoreticular MOFs and their application in methane storage. *Science* **295** (5554), 469–472.

El-Khaiary, M. I. & Malash, G. F. 2011 Common data analysis errors in batch adsorption studies. *Hydrometallurgy* **105** (3–4), 314–320.

Fang, Y., Ma, Y., Zheng, M., Yang, P., Asiri, A. M. & Wang, X. 2018 Metal–organic frameworks for solar energy conversion by photoredox catalysis. *Coordination Chemistry Reviews* **373**, 83–115.

Gu, Z., Gao, M., Luo, Z., Xue, G., Lu, L. & Liu, Y. 2014 Gemini surfactant modified montmorillonite as highly efficient adsorbent for anionic dyes. *Separation Science and Technology* **49** (18), 2878–2889.

Haddad, D., Mellah, A., Nibou, D. & Khemaissia, S. 2018 Promising enhancement in the removal of uranium ions by surface-modified activated carbons: kinetic and equilibrium studies. *Journal of Environmental Engineering* **144** (5), 4018027.

Hafizovic, J., Bjørgen, M., Olsbye, U., Dietzel, P. D. C., Bordiga, S., Prestipino, C., Lamberti, C. & Lillerud, K. P. 2007 The inconsistency in adsorption properties and powder XRD data of MOF-5 is rationalized by framework interpenetration and the presence of organic and inorganic species in the nanocavities. *Journal of the American Chemical Society* **129** (12), 3612–3620. https://doi.org/10.1021/ja0675447.

Haque, E., Jun, J. W. & Jhung, S. H. 2011 Adsorptive removal of methyl orange and methylene blue from aqueous solution with a metal-organic framework material, iron terephthalate (MOF-235). *Journal of Hazardous Materials* **185** (1), 507–511.

Haque, E., Lee, J. E., Jang, I. T., Hwang, Y. K., Chang, J.-S., Jegal, J. & Jhung, S. H. 2010 Adsorptive removal of methyl orange from aqueous solution with metal-organic frameworks, porous chromium-benzenedicarboxylates. *Journal of Hazardous Materials* **181** (1–3), 535–542.

Haque, E., Lo, V., Minett, A. I., Harris, A. T. & Church, T. L. 2014 Dichotomous adsorption behaviour of dyes on an amino-functionalised metal–organic framework, amino-MIL-101 (Al). *Journal of Materials Chemistry* **A 2** (1), 193–203.

Inglezakis, V. J. 2007 Solubility-normalized Dubinin–Astakhov adsorption isotherm for ion-exchange systems. *Microporous and Mesoporous Materials* **103** (1–3), 72–81.

Iswarya, N., Kumar, M. G., Rajan, K. S. & Balaguru, R. J. B. 2012 Synthesis, characterization and adsorption capability of MOF-5. *Asian Journal of Scientific Research* **5** (4), 247–254.

Jiang, N., Deng, Z., Liu, S., Tang, C. & Wang, G. 2016 Synthesis of metal organic framework (MOF-5) with high selectivity for CO_2/N_2 separation in flue gas by maximum water concentration approach. *Korean Journal of Chemical Engineering* **33** (9), 2747–2755.

Karthikeyan, S., Sivakumar, B. & Sivakumar, N. 2010 Film and pore diffusion modeling for adsorption of Reactive red 2 from aqueous solution on to activated carbon prepared from bio-diesel industrial waste. *Journal of Chemistry* **7** (S1), S175–S184.

Khan, N. A., Hasan, Z. & Jhung, S. H. 2013 Adsorptive removal of hazardous materials using metal-organic frameworks (MOFs): a review. *Journal of Hazardous Materials* **244**, 444–456.

Laib, R., Amokrane-Nibou, S., Nibou, D. & Trari, M. 2019 Recovery of recycled paper in the removal of the textile dye Basic yellow 28: characterization and adsorption studies. *Nordic Pulp & Paper Research Journal* **34** (2), 218–227.

Lee, Y.-R., Kim, J. & Ahn, W.-S. 2013 Synthesis of metal-organic frameworks: a mini review. *Korean Journal of Chemical Engineering* **30** (9), 1667–1680.

Mekatel, E. H., Amokrane, S., Aid, A., Nibou, D. & Trari, M. 2015 Adsorption of methyl orange on nanoparticles of a synthetic zeolite NaA/CuO. *Comptes Rendus Chimie* **18** (3), 336–344.

Mekatel, E., Amorkrane, S., Trari, M., Nibou, D., Dahdouh, N. & Ladjali, S. 2019 Combined adsorption/photocatalysis process for the decolorization of Acid Orange 61. *Arabian Journal for Science and Engineering* **44** (6), 5311–5322.

Michael, I., Rizzo, L., McArdell, C. S., Manaia, C. M., Merlin, C., Schwartz, T., Dagot, C. & Fatta-Kassinos, D. 2013 Urban wastewater treatment plants as hotspots for the release of antibiotics in the environment: a review. *Water Research* **47** (3), 957–995.

Mittal, A., Malviya, A., Kaur, D., Mittal, J. & Kurup, L. 2007 Studies on the adsorption kinetics and isotherms for the removal and recovery of Methyl Orange from wastewaters using waste materials. *Journal of Hazardous Materials* **148** (1–2), 229–240.

Mu'azu, N. D., Jarrah, N., Zubair, M., Manzar, M. S., Kazeem, T. S. & Al-Harthi, M. 2019 Evaluation of novel Mg/Al/Ni-BaFe ternary layered hydroxides uptake of methyl orange dye from water. *Korean Journal of Chemical Engineering* **36** (12), 2008–2022.

Mueller, U., Schubert, M., Teich, F., Puetter, H., Schierle-Arndt, K. & Pastre, J. 2006 Metal–organic frameworks – prospective industrial applications. *Journal of Materials Chemistry* **16** (7), 626–636.

Phan, N. T. S., Le, K. K. A. & Phan, T. D. 2010 MOF-5 as an efficient heterogeneous catalyst for Friedel–Crafts alkylation reactions. *Applied Catalysis A: General* **382** (2), 246–253.

Ramanayaka, S., Vithanage, M., Sarmah, A., An, T., Kim, K.-H. & Ok, Y. S. 2019 Performance of metal–organic frameworks for the adsorptive removal of potentially toxic elements in a water system: a critical review. *RSC Advances* **9** (59), 34359–34376.

Rodríguez, N. A., Parra, R. & Grela, M. A. 2015 Structural characterization, optical properties and photocatalytic activity of MOF-5 and its hydrolysis products: implications on their excitation mechanism. *RSC Advances* **5** (89), 73112–73118.

Simonin, J.-P. 2016 On the comparison of pseudo-first order and pseudo-second order rate laws in the modeling of adsorption kinetics. *Chemical Engineering Journal* **300**, 254–263.

Singh, K. & Arora, S. 2011 Removal of synthetic textile dyes from wastewaters: a critical review on present treatment technologies. *Critical Reviews in Environmental Science and Technology* **41** (9), 807–878.

Suteu, D. & Malutan, T. 2013 Industrial cellolignin wastes as adsorbent for removal of methylene blue dye from aqueous solutions. *BioResources* **8** (1), 427–446.

Tan, K., Nijem, N., Gao, Y., Zuluaga, S., Li, J., Thonhauser, T. & Chabal, Y. J. 2015 Water interactions in metal organic frameworks. *CrystEngComm* **17** (2), 247–260.

Tsibranska, I. & Hristova, E. 2011 Comparison of different kinetic models for adsorption of heavy metals onto activated carbon from apricot stones. *Bulgarian Chemical Communications* **43** (3), 370–377.

Vargas, A. M. M., Cazetta, A. L., Kunita, M. H., Silva, T. L. & Almeida, V. C. 2011 Adsorption of methylene blue on activated carbon produced from flamboyant pods (Delonix regia): study of adsorption isotherms and kinetic models. *Chemical Engineering Journal* **168** (2), 722–730.

Wakkel, M., Khiari, B. & Zagrouba, F. 2019 Textile wastewater treatment by agro-industrial waste: equilibrium modelling, thermodynamics and mass transfer mechanisms of cationic dyes adsorption onto low-cost lignocellulosic adsorbent. *Journal of the Taiwan Institute of Chemical Engineers* **96**, 439–452.

Wang, H., Duan, M., Guo, Y., Wang, C., Shi, Z., Liu, J. & Lv, J. 2018 Graphene oxide edge grafting of polyaniline nanocomposite: An efficient adsorbent for methylene blue and methyl orange. *Water Science and Technology* **77** (12), 2751–2760. https://doi.org/10.2166/wst.2018.250.

Wood, G. O. 2001 Affinity coefficients of the Polanyi/Dubinin adsorption isotherm equations: a review with compilations and correlations. *Carbon* **39** (3), 343–356.

Wu, F.-C., Tseng, R.-L. & Juang, R.-S. 2009 Characteristics of Elovich equation used for the analysis of adsorption kinetics in dye-chitosan systems. *Chemical Engineering Journal* **150** (2–3), 366–373.

Zhang, J., Liu, M., Yang, T., Yang, K. & Wang, H. 2017 Synthesis and characterization of a novel magnetic biochar from sewage sludge and its effectiveness in the removal of methyl orange from aqueous solution. *Water Science and Technology* **75** (7), 1539–1547. doi:10.2166/wst.2017.014.

Zhang, H.-Y., Yang, C., Geng, Q., Fan, H.-L., Wang, B.-J., Wu, M.-M. & Tian, Z. 2019 Adsorption of hydrogen sulfide by amine-functionalized metal organic framework (MOF-199): an experimental and simulation study. *Applied Surface Science* **497**, 143815.

First received 16 August 2020; accepted in revised form 13 November 2020. Available online 27 November 2020